

Structural ordering and enhanced carrier mobility in organic polymer thin film transistors

L. Kinder^{a,*}, J. Kanicki^{a,b}, P. Petroff^a

^a *Materials Department, University of California Santa Barbara, Santa Barbara, CA 93106, USA*

^b *EECS Department, University of Michigan, Ann Arbor, MI 48109-2108, USA*

Received 11 June 2004; received in revised form 30 June 2004; accepted 30 June 2004

Available online 20 August 2004

Abstract

We have used thermal treatment and rubbed polyimide alignment layers to produce large domains of poly(9,9-dioctylfluorene-co-bithiophene) alternating copolymer (F8T2). The direction of rubbing on the polyimide surface determines the orientation of these domains, allowing us to create thin-film transistors with channel lengths parallel and perpendicular to the liquid–crystal polymer director. We show that thermal annealing at 280 °C brings F8T2 into a mesophase as observed by X-ray diffraction and differential scanning calorimetry. Polarized optical microscopy and polarized UV–vis absorption spectroscopy show that this ordered phase is associated with very large ordered domains and corresponds to a thermotropic, nematic liquid–crystal phase. We investigated thermal annealing effects on both F8T2 structural ordering and the associated anisotropic electrical properties of the thin-film transistors (TFTs). Enhanced mobility of holes is observed with ordering. Field-effect mobility parallel to the polymer backbone is as much as 6.5 times greater than the perpendicular configuration.

© 2004 Elsevier B.V. All rights reserved.

Keywords: Organic semiconductor; Liquid–crystal; Transistor; Thiophene; Fluorene; Absorption

1. Introduction

The importance of main-chain alignment for enhancement of specific electronic properties of organic polymer thin-film transistors (OP-TFTs) is widely recognized [1–5]. In a single isolated polymer chain, carrier conduction occurs only along the conjugated polymer chain backbone (intramolecular transport). For the three-dimensional polymer structure, carrier transport occurs not only along the chains, but also between the neighbor chains (intermolecular transport). It is generally believed that this intermolecular transport occurs via a hopping or tunneling mechanism dependent on molecular separation distances such that better packing of polymer chains and elimination of grain boundary defects enhance interchain transfer rates [6,7]. Hence, the structural ordering

in an intrinsic organic polymer semiconductor can have a pronounced influence on charge transport in OP-TFTs.

Here, we rely on the self-aligning nature of liquid crystals to produce aligned thin semiconducting films. Through heat treatment in nitrogen environment, the semiconductor is brought into the mesophase, where better chain packing occurs. To eliminate grain boundaries, we fabricate monodomain films by orienting the liquid–crystal director with polyimide surface alignment layers. The relationship between the structural ordering of F8T2 and OP-TFT electrical properties is investigated by fabricating transistors on aligned F8T2 films. We observe that charge transport is anisotropic. The highest field-effect mobilities occur when long polymer molecules are aligned with backbones lying in the direction of current flow. In this orientation, there are more conduction paths, and diffusion of carriers is greatest. In the parallel alignment, field-effect mobility values are 2–3 times greater than mobility for as-deposited (amorphous)

* Corresponding author.

E-mail address: lkinder@engineering.ucsb.edu (L. Kinder).

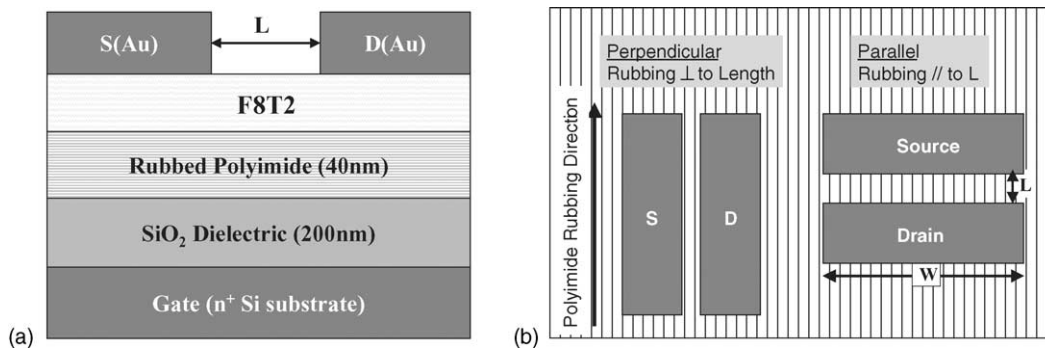


Fig. 1. Thin-film transistor structure: (a) cross-section and (b) top view.

films, and 4–6 times greater than values obtained for devices with channel lengths perpendicular to polymer chain alignment. Thus, we establish that thermal treatment and texturing of the organic polymer is an effective method for achieving macroscopic ordering and enhanced mobility in F8T2 TFTs.

2. Materials and methods

Poly(9,9-dioctylfluorene-co-bithiophene) alternating copolymer (F8T2) has several properties which make it convenient for studying electrical characteristics of aligned polymer films: conjugated segments for charge transport, relatively high stability in air, solubility in a wide range of solvents, and thermotropic liquid crystallinity which allows better packing via self-assembly. F8T2 is a main-chain liquid-crystal polymer of the ‘hairy-rod’ type (see inset in Fig. 2). The octyl side chains protruding from the rod-like backbone (hence the name ‘hairy-rod’) facilitate solvation.

F8T2 polymers supplied by Dow Chemical were synthesized with various conditions and thus had various molecular weights and polydispersity, properties that can influence mobility, morphology, transition temperatures, and degree of alignment [8]. Weight average and number average molecular weights (M_w and M_n , respectively) were determined from tetrahydrofuran solutions by gel permeation chromatography (GPC) using polystyrene equivalents. All results presented here are obtained using a polymer with $M_w = 31.3$ kg/mol and polydispersity, $PDI = M_w/M_n = 2.1$. This polymer was chosen because it had the lowest polydispersity of all F8T2 materials supplied. Thermogravimetric analysis (TGA) shows that F8T2 has a high decomposition temperature ($>400^\circ\text{C}$), suitable for transistor fabrication and operation.

Thin films were deposited from 10 mg/mL (1%) xylenes solutions onto glass or transistor substrates using spin- or drop-casting techniques and were immediately vacuum-annealed at 110°C to remove solvents. Further thermal treatment to obtain the liquid-crystal phase was performed under nitrogen purge. It has been shown that long-range ordering of F8T2 can be attained using polyimide alignment layers on

substrate surfaces *prior* to F8T2 deposition [9,10]. Diluted polyimides from Nissan Chemical (RN-1340) were spun onto glass or transistor substrates, baked to imidization at 280°C for 45 min and either hand-rubbed with a Yoshikawa rayon cloth (for formation of aligned films) or left without grooves for comparison. Polyimide thickness is 40 nm as determined by ellipsometry and Dektak Profilometer. F8T2 is cast on top of these rubbed or unrubbed polyimide layers, and then the thermal treatment is performed.

Electrical analysis is done using the thin-film field-effect transistor structure shown in Fig. 1a. The schematic shows that a heavily n+ doped silicon substrate serves as a common back gate, although a finite size gate structure would be preferred since capacitive charging occurs between the source and drain electrodes and the gate terminal. The gate dielectric layer is composed of a thermal SiO_2 (200 nm) layer in series with the rubbed polyimide alignment layer. Gold source and drain contacts are defined by photolithography on top of the polymer with a mask allowing for fabrication of devices with parallel and perpendicular channel lengths to be formed on the same sample (Fig. 1b). Channels have length (L) of 5–40 μm and width (W) of 500 or 1000 μm .

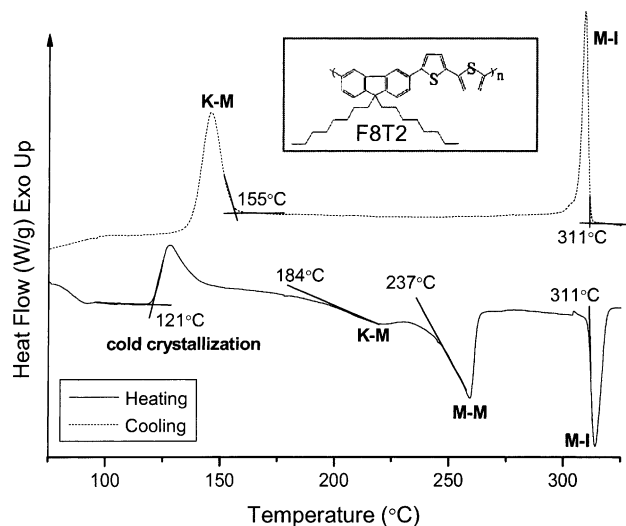


Fig. 2. DSC curves for F8T2. Inset shows the chemical structure of F8T2.

3. Structural analysis

Thermotropic transitions in large molecular weight main chain polymers are difficult to identify due to the rarity of monotropic mesomorphism and decreased definition of the mesophase texture under the optical microscope. Generally, a combination of techniques is employed for phase identification. Here we use differential scanning calorimetry (DSC) as a primary method to detect transitions. We confirm the DSC analysis with X-ray diffraction and polarized optical microscopy (POM) methods.

DSC curves of F8T2 in the first heating and cooling cycles at scanning rates of $10\text{ }^{\circ}\text{C}/\text{min}$ in N_2 are shown in Fig. 2. Phase changes are accompanied by a release or intake of thermal energy represented by peaks and dips in the DSC scan. When F8T2 is heated, the material undergoes a glass transition followed by cold crystallization onset at $121\text{ }^{\circ}\text{C}$. Melting of the solid (K) occurs between 184 and $265\text{ }^{\circ}\text{C}$. In this region, two peaks are observed, which could indicate the complexity of melting in a polymer chain material or the existence of two distinct mesophase (M) states. At these temperatures, thin films of F8T2 become birefringent, brightening the image observed through crossed polarizers, as regions of molecules with preferred orientation in the substrate plane rotate the incoming light such that it is not cancelled by a second polarizer (analyzer). Observation of birefringence in POM implies a mesophase with homogenous alignment (F8T2 backbones lie in the plane of the substrate rather than perpendicular to the surface as is seen in homeotropic alignment). The mesophase–isotropic (M–I) transition occurs at $311\text{ }^{\circ}\text{C}$, bringing the material to a disordered, liquid phase and

corresponding loss of birefringence in POM. Upon cooling the isotropic liquid, the mesophase–isotropic phase transition is reversible ($311\text{ }^{\circ}\text{C}$) while notable super-cooling is observed for the solid–mesophase transition ($155\text{ }^{\circ}\text{C}$). Being prone to super-cooling, the material can be frozen from the mesophase to form a nematic glass at room temperature. It is common for the crystal–crystal and crystal–mesophase transitions of liquid crystals to exhibit super-cooling in the cooling cycle, while the mesophase–mesophase and mesophase–isotropic liquid–crystal transitions occur at only slightly different temperatures on cooling and heating.

Powder X-ray diffraction shows that structural changes occur at phase transition temperatures identified with DSC and POM. In Fig. 3, we show X-ray diffraction scans taken at temperatures ranging from 30 to $340\text{ }^{\circ}\text{C}$ of an unoriented F8T2 sample. X-ray scans were performed in reflection using a Philips XPERT MPD Diffractometer at angles $2\theta = 4\text{--}20^{\circ}$ and power of $40\text{ kV}/30\text{ mA}$. Scans at elevated temperatures ($150\text{--}340\text{ }^{\circ}\text{C}$) were obtained by heating to temperature with a Pt hot stage and holding temperature during data collection. All heating and scanning was performed in N_2 environment.

X-ray data show that prior to heating, the F8T2 is in a disordered state with a broad peak centered around $4\text{--}6\text{ \AA}$ which corresponds to average intermolecular spacing. X-ray data at $150\text{ }^{\circ}\text{C}$ suggest the occurrence of cold crystallization by the emergence of a layering peak and the sharpening of large angle peaks. The 2θ peak at $\sim 5.5^{\circ}$ corresponds to a layering distance, $d_{100} = 16\text{ \AA}$, between sheets of F8T2 chains which pack in a plane perpendicular to their longitudinal axes. This lamellar structure appears due to the segregation of main chain backbones from the aggregated alkyl side chains.

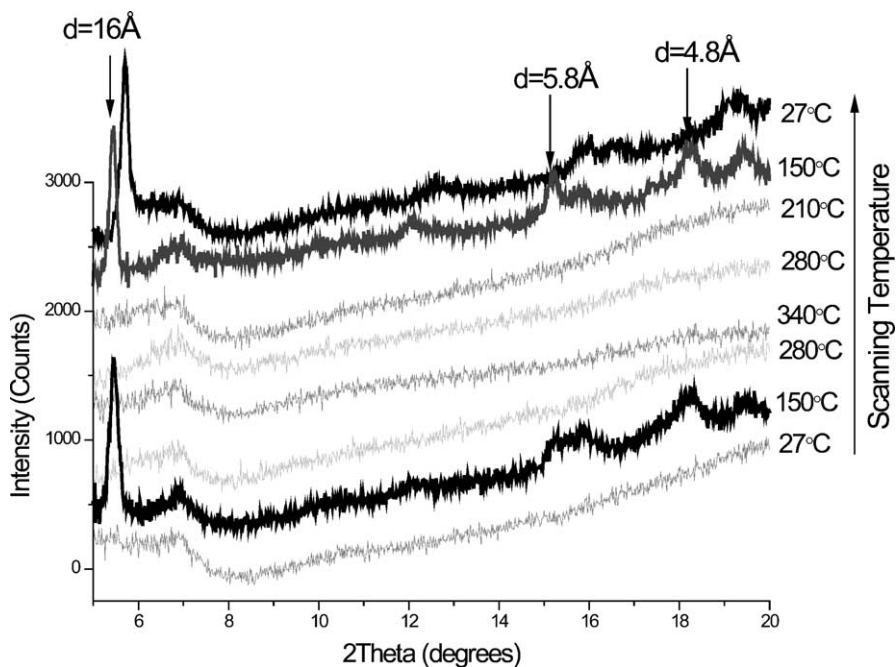


Fig. 3. X-ray scans at temperatures (from bottom to top) 27 , 150 , 280 , 340 , 280 , 210 , 150 , $27\text{ }^{\circ}\text{C}$ as indicated for each scan. Plots are offset vertically to show development of 2θ peaks.

Smaller, broader peaks corresponding to spacings of 4.8 and 5.8 Å arise from ordering within the layer planes. This ordering could be due to the lateral distance between polymer chains within the layer. Similar coplanar arrangement of aromatic backbones within layers is observed for polyesters and polyamides with alkyl chains [11,12]. Alternatively, these small peaks could arise from side-chain crystallization [13].

The next X-ray scan taken at 280 °C shows that heating to the mesophase results in an expected loss of order and the corresponding disappearance of all peaks except for the broad, large-angle peak seen at room temperature. These results are expected for nematic main-chain liquid-crystal polymers. X-ray scans in the isotropic phase (340 °C) and upon cooling to the mesophase (280 and 210 °C) display similar curves. Ordering peaks return when the sample is cooled to mesophase–solid transition (150 °C) and is maintained at room temperature.

X-ray and POM results discussed above are obtained from unoriented F8T2 copolymer. Annealing these samples creates liquid crystalline domains, but films lack long-range ordering since individual domains are not all oriented in a specific direction. When F8T2 is deposited on rubbed polyimide surfaces, well-ordered, monodomain films can be made. Before heat treatment, the spin-cast material shows no signs of ordering—it is not birefringent under POM, there are no ordering peaks observed in X-ray, and UV–vis spectroscopy shows that light polarized parallel to the rubbing direction is as strongly absorbed as perpendicularly polarized light. When this sample is heated to 280 °C, nematic domains and thread-like defects appear in POM images (Fig. 4a). Holding this temperature for 10 min anneals out the defects, leaving a mesophase domain that is much larger than the size of a transistor channel (Fig. 4b). After quenching from the

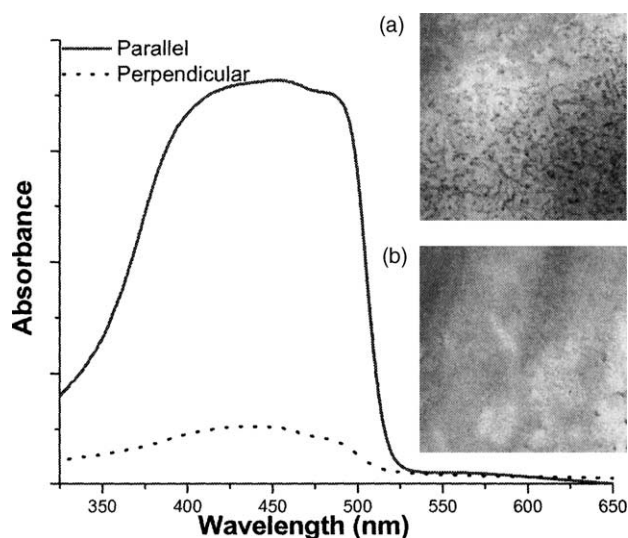


Fig. 4. F8T2 absorption of UV–vis light polarized parallel and perpendicular to rubbing direction. Experiment performed after quenching F8T2 from the mesophase. Inset: optical micrograph (250 nm × 250 nm) of surface under crossed polarizers (a) upon reaching 280 °C and (b) after 10 min anneal at 280 °C.

mesophase, the sample is analyzed with polarized UV–vis spectroscopy and we observe that the sample has a dichroic ratio (absorption_∥: absorption_⊥) of 11, indicating strong alignment in the rubbing direction (Fig. 4). One explanation for the F8T2 alignment is that through rubbing, the polyimide is shear-aligned, forming a template for liquid-crystal alignment such that F8T2 molecules close to the interface lie with their long axes along the rubbing direction and neighboring molecules align with these underlying molecules when heated to the mesophase [14].

4. Electrical analysis

To investigate the relationship between structural and electrical properties in F8T2, we fabricate OP-TFTs with device structure shown in Fig. 1. Transistor contacts are oriented such that on the same F8T2 film, current flow parallel and perpendicular to the alignment direction can be probed. Fig. 5 shows output characteristics for perpendicularly oriented devices. ∥ indicates that the device channel length (L) is parallel to the polyimide rubbing direction whereas ⊥ indicates that L is perpendicular to the rubbing (Fig. 1b). Negative signs of drain current (I_{ds}) under negative drain voltage (V_{ds}) and gate voltage (V_{gs}) indicate hole transport and a p-type F8T2 semiconductor. These devices operate in the accumulation mode, turning on as gate bias is negatively increased ($V_{gs} = 0$ to -20 V). At low V_{ds} , the drain current I_{ds} increases linearly, indicating good charge injection from the source and drain contacts. There is a clearly defined linear regime at $V_{ds} < V_{gs}$ followed by saturation regime at $V_{ds} > V_{gs}$ for each gate voltage. Output characteristics are sensitive to the chain orientation. When polymer backbones are aligned with the current flow (∥ configuration), more conduction paths are available to transport charges. Fig. 5 shows that the parallel saturation current is ~ 4 times greater than the perpendicular saturation current.

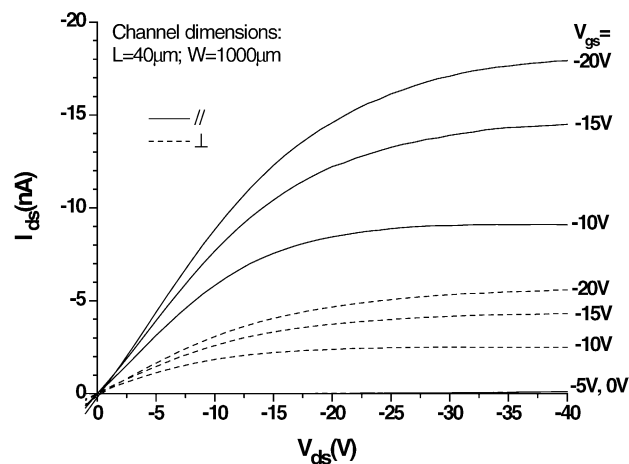


Fig. 5. Output characteristics (I_{ds} – V_{ds}) at $V_{gs} = 0$ to -20 V for perpendicularly oriented devices.

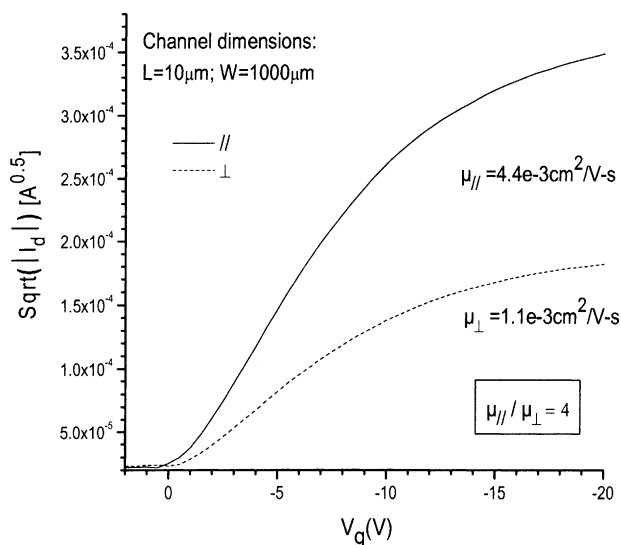


Fig. 6. Transfer characteristics of perpendicularly oriented devices in the saturation regime ($V_{ds} = -50$ V). Hole mobility is anisotropic, $\mu_{||}/\mu_{\perp} = 4$.

The saturation of I_{ds} due to the pinch-off of the accumulation layer occurs when $-V_{ds} > -(V_g - V_t)$, where V_t is the threshold voltage. In the saturation regime, I_{ds} is modeled with the standard TFT equation [15]:

$$I_{ds} = \frac{W}{2L} \mu C_i (V_g - V_t)^2$$

where C_i is the capacitance of the dual-layer dielectric as calculated from the dielectric constant and thickness measured from the polyimide and silicon oxide layers. Fig. 6 shows saturation regime transfer characteristics of the same device as in Fig. 5. The hole field-effect mobility (μ) can be calculated from the slope of the plot of $\sqrt{I_{ds}}$ versus V_g . The mobility calculated in the saturation regime was $4.4 \times 10^{-3} \text{ cm}^2/(\text{V s})$ for the parallel configuration and only $1.1 \times 10^{-3} \text{ cm}^2/(\text{V s})$ for the perpendicular case, yielding a mobility anisotropy ratio ($\mu_{||}/\mu_{\perp}$) of 4. This corresponds to the anisotropy of saturation current observed in Fig. 5.

Several transistors were studied and devices with parallel alignment consistently out-performed perpendicular devices, showing higher values of μ and saturation current. For the parallel configuration, saturation mobilities ranged from 2×10^{-3} to $1 \times 10^{-2} \text{ cm}^2/(\text{V s})$, and the mobility anisotropy ratio ($\mu_{||}/\mu_{\perp}$) ranged from 3.5 to as large as 6.5.

Amorphous devices, which are deposited on rubbed polyimide alignment layers but not thermally treated, have mobility values in-between those of the parallel and perpendicular films. Enhancement of device performance is observed when interchain charge transport is facilitated by ordering the film in the mesophase (which improves chain packing and reduces the number of grain boundary defects) and aligning the director of this nematic liquid–crystal in the direction of current flow.

5. Conclusions

We have conducted structural and electrical analysis of ordered F8T2 films. Combining techniques of POM, DSC and X-ray diffraction, we observe that F8T2 enters a nematic liquid–crystal phase at elevated temperatures. The liquid–crystal director can be oriented using rubbed polyimide alignment layers, allowing production of monodomain devices. A dichroic ratio of 11 is observed with polarized UV–vis spectroscopy of films that have been quenched from the aligned mesophase to room temperature, demonstrating preservation of the alignment and a nematic glass structure. We demonstrate that this alignment method is compatible with processing. Photolithography is used to define source and drain contacts on top of the F8T2 film without affecting its alignment capability. OP-TFTs with aligned F8T2 layers show that the hole mobility is anisotropic with ratios, $\mu_{||}/\mu_{\perp}$, up to 6.5. We observe a relationship between structural and electrical properties in F8T2 films, showing that proper processing leads to enhanced mobility.

Acknowledgements

This work was supported equally by the MRSEC Program of the National Science Foundation under Award No. DMR00-80034 and by the MARCO Agreement 2003-NT-1107. Dow Chemical Company supplied polyfluorene materials. We thank J. Swensen for technical assistance and A. Hexemer, A. Heeger, and E. Kramer for helpful discussions.

References

- [1] F. Garnier, A. Yassar, R. Hajlaoui, G. Horowitz, F. Deloffre, B. Servet, S. Ries, P. Alnot, *J. Am. Chem. Soc.* 115 (1993) 8716.
- [2] F. Garnier, G. Horowitz, D. Fichou, A. Yassar, *Supramol. Sci.* 4 (1997) 155.
- [3] Z. Bao, *Adv. Mater.* 12 (2000) 227.
- [4] X.L. Chen, A.J. Lovinger, Z. Bao, J. Sapjeta, *Chem. Mater.* 13 (2001) 1341.
- [5] H. Sirringhaus, R.J. Wilson, R.H. Friend, M. Inbasekaran, W. Wu, E.P. Wu, M. Grell, D.D.C. Bradley, *Appl. Phys. Lett.* 77 (2000) 406.
- [6] M. Pope, C.E. Swenberg, *Electronic Properties in Organic Crystals*, Oxford University, New York, 1982.
- [7] Z.H. Wang, E.M. Scherr, A.G. MacDiarmid, A.J. Epstein, *Phys. Rev. B* 45 (1992) 4190.
- [8] A. Ciferri, *Liquid Crystallinity in Polymers*, VCH Publishers, New York, 1991.
- [9] M. Grell, M. Redecker, K.S. Whitehead, D.D.C. Bradley, M. Inbasekaran, E.P. Wu, W. Wu, *Liq. Cryst.* 26 (1999) 1403.
- [10] G. Lieser, M. Oda, T. Miteva, A. Meisel, H. Nothofer, U. Scherf, *Macromolecules* 33 (2000) 4490.
- [11] L. Cervinka, M. Ballauff, *Colloid. Polym. Sci.* 270 (1992) 859.
- [12] R. Stern, M. Ballauff, G. Lieser, G. Wegner, *Polymer* 32 (1991) 2096.
- [13] S. Kawana, M. Durrell, J. Lu, J.E. Macdonald, M. Grell, D.D.C. Bradley, P.C. Jukes, R.A.L. Jones, S.L. Bennett, *Polymer* 43 (2002) 1907.
- [14] J.M. Geary, J.W. Goodby, A.R. Kmetz, J.S. Patel, *J. Appl. Phys.* 62 (1987) 4100.
- [15] G. Horowitz, *Adv. Mater.* 10 (1998) 365.